

 Open access • Posted Content • DOI:10.1101/2021.07.07.451322

Pre-trial predictors of conflict response efficacy in human dorsolateral prefrontal cortex — [Source link](#)

[Alexander B. Herman](#), [Elliot H. Smith](#), [Mark Yates](#), [Guy M. McKhann](#) ...+3 more authors

Institutions: [University of Minnesota](#), [Columbia University](#), [Baylor College of Medicine](#)

Published on: 09 Jul 2021 - [bioRxiv](#) (Cold Spring Harbor Laboratory)

Topics: [Dorsolateral prefrontal cortex](#)

Related papers:

- [Task-dependent response conflict monitoring and cognitive control in anterior cingulate and dorsolateral prefrontal cortices.](#)
- [Conflict effects without conflict in anterior cingulate cortex: multiple response effects and context specific representations.](#)
- [Right ventrolateral prefrontal cortex mediates individual differences in conflict-driven cognitive control](#)
- [Dynamic adjustments of cognitive control: Oscillatory correlates of the conflict adaptation effect](#)
- [Observed and self-experienced conflict induce similar behavioral and neural adaptation](#)

Share this paper:    

View more about this paper here: <https://typeset.io/papers/pre-trial-predictors-of-conflict-response-efficacy-in-human-2p4wsv5ei7>

Pre-trial predictors of conflict response efficacy in human dorsolateral prefrontal cortex

Alexander B. Herman^{1†}, Elliot H. Smith^{2,4},
Catherine A. Schevon⁴, Mark Yates⁵, Guy M. McKhann⁵,
Matthew Botvinick⁶, Benjamin Y. Hayden^{7*}, and Sameer Anil Sheth^{8*}

1. Department of Psychiatry, University of Minnesota, Minneapolis, MN, 55455, USA
2. Department of Neurosurgery, University of Utah, Salt Lake City, UT, 84132, USA
3. Department of Psychiatry, Columbia University, and New York State Psychiatric Institute, New York, NY, 10032, USA
4. Department of Neurology, Columbia University, NYC, NY, USA 10027
5. Department of Neurological surgery, Columbia University, NYC, NY, USA 10027
6. DeepMind, London, UK
7. Department of Neuroscience, Center for Magnetic Resonance Research, and Center for Neural Engineering, University of Minnesota, Minneapolis, MN, 55455, USA
8. Department of Neurosurgery, Baylor College of Medicine, Houston, TX, 77030, USA

* These two authors contributed equally.

† Lead contact

Keywords: coding dimension, dorsolateral prefrontal cortex, cognitive control, conflict, anterior cingulate cortex

Acknowledgements: This work was supported by NIH R01 MH106700, NIH U01 NS108923, NIH K12 NS080223, NIH S10 OD018211, NIH R01 NS084142, NIH R01 DA038615, the Brain and Behavior Foundation, and the Dana Foundation. This work was also supported by the Center for Neuroengineering (CNE) at UMN. Special thanks to Camilla Casadei, David K. Peprah, and Timothy G. Dyster for coordination and data collection efforts. The funders had no role in study design, data collection and analysis, decision to publish, or preparation of the manuscript.

ABSTRACT

37
38
39
40
41
42
43
44
45
46
47
48
49
50
51
52
53
54
55
56
57

The ability to perform motor actions depends, in part, on the brain's initial state, that is, the ensemble firing rate pattern prior to the initiation of action. We hypothesized that the same principle would apply to cognitive functions as well. To test this idea, we examined a unique set of single unit data collected in human dorsolateral prefrontal (dlPFC) cortex. Data were collected in a conflict task that interleaves Simon (motor-type) and Eriksen (flanker-type) conflict trials. In dlPFC, variability in pre-trial firing rate predicted the ability to resolve conflict, as inferred from reaction times. Ensemble patterns that predicted faster Simon reaction times overlapped slightly with those predicting Erikson performance, indicating that the two conflict types are associated with near-orthogonal initial states, and suggesting that there is a weak abstract or amodal conflict preparatory state in this region. These codes became fully orthogonalized in the response state. We interpret these results in light of the initial state hypothesis, arguing that the firing patterns in dlPFC immediately preceding the start of a task predispose it for the efficient implementation of cognitive action.

INTRODUCTION

58
59 The ability to respond effectively to a stimulus can depend on the state of the brain even
60 before the stimulus appears¹⁻³. In other words, our responses are determined not only by the
61 neural activity driven by the response-driving stimulus, but by the way that activity interacts with
62 ongoing neural activity⁴. In the motor system, one expression of this idea is the *initial state*
63 *hypothesis*, which holds that motor control involves a series of dynamical states and that
64 initiation of motor control requires a particular state⁵⁻¹⁰. Variability in performance, typically
65 assessed with reaction times, corresponds in part to variability in pre-trial firing rates because
66 those reflect the response of the system relative to the optimal response-driving initial state. We
67 and others have proposed that dynamical principles relevant to the motor system may apply to
68 non-motor processes, including higher level cognitive processes¹¹⁻¹⁵. We hypothesized,
69 therefore, that the ability to implement a cognitive process may likewise depend on the initial
70 state of the system.

71 We are particularly interested in conflict detection and resolution, a pair of
72 complementary and relatively well-studied cognitive behaviors whose neuronal basis is
73 beginning to be understood¹⁶⁻²¹. Conflict typically refers to a competition between possible
74 stimuli for attention and/or action and generally evokes slower reaction times, increased error
75 rates, and disengagement from alternative tasks^{22,23}. This refocusing of mental resources is the
76 basis of conflict resolution and presumably occurs in response to an internal detection of conflict
77 and generation and propagation of a conflict signal. We hypothesized that the ability to deal
78 effectively with conflict depends in part on variability in neural processes in conflict-relevant
79 brain regions before the appearance of the conflicting stimuli.

80 The dorsolateral prefrontal cortex (dlPFC) is among the most studied brain regions for
81 cognitive control, along with anterior cingulate cortex^{16,20,24-26}. dlPFC shows systematic changes
82 in hemodynamic response, local field potential (LFP), and firing rate in the face of conflict
83 (*ibid.*). We have recently proposed that these two regions play somewhat distinct, albeit
84 complementary roles in conflict detection and resolution¹⁶. We proposed that dlPFC is more
85 associated with implementation, and thus potentially a closer cognitive analogue to motor areas
86 (see also²⁵⁻²⁷).

87 Here, we examined firing rates of single neurons in dlPFC while humans performed the
88 multi-source interference task (MSIT), a task that manipulates two different forms of conflict, a
89 motor (Simon) type and a perceptual (Eriksen flanker) type^{16,19}. We found that activity patterns
90 in the period preceding the start of the trial predicted reaction time in dlPFC, even after
91 regressing out prior trial reaction time and conflict type. At the individual cell level, we found
92 evidence for a neural code for response times specific to each conflict type. These codes
93 overlapped slightly but significantly at the population level, indicating the presence of a weak
94 shared conflict-amodal code. These results endorse the idea that conflict resolution reflects the
95 interaction between stimulus-driven activity and ongoing fluctuations in pre-trial activity,
96 support the initial state hypothesis for cognitive actions, and suggests a mechanism by which the
97 brain can respond both flexibly and efficiently to different conflict conditions.

98
99
100
101
102

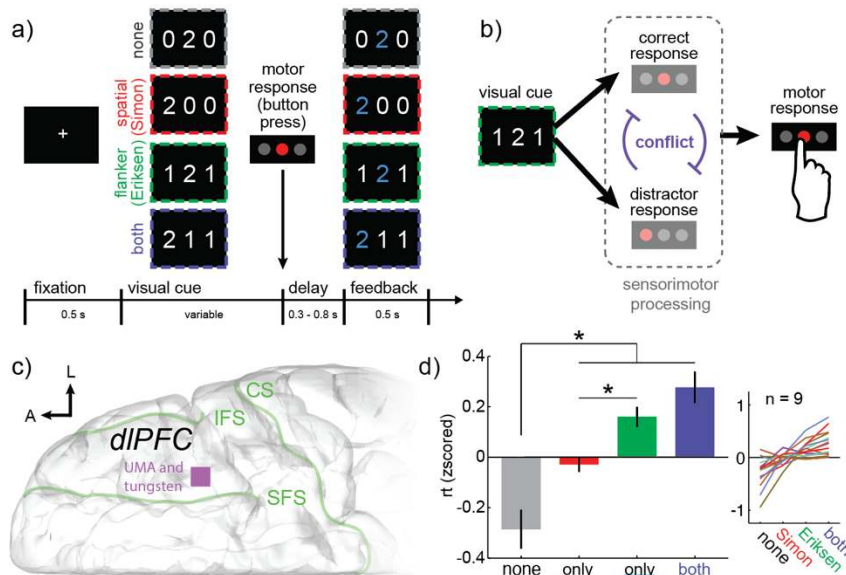
103
104
105
106
107
108
109
110
111
112
113
114
115
116
117
118
119
120
121
122
123

RESULTS

Behavior

We examined responses of single neurons recorded in dlPFC in 9 human patients (**Figure 1A**). Task-related responses in this dataset were described in an earlier study, but pre-trial responses, the focus of the present study, were not analyzed^{16,28}. Participants performed the multi-source interference task (MSIT), a task that involves two independently manipulated types of conflict (**Figure 1B**).

The validity of this task as a manipulation of conflict has been demonstrated^{16,19,29,30}. We therefore only briefly summarize the evidence that the task manipulates conflict. Most importantly, median reaction time in the Simon trials (1.5 sec) was significantly slower than no conflict trials (1.26 sec, $p=0.017$, $z=2.402$, ranksum=8438). Likewise, reaction times in the Eriksen trials (1.63 sec) was slower than in no conflict trials ($p<0.001$, $z=4.51$, ranksum=259). Finally, reaction times on both-conflict trials (1.71 sec) were longer than on Simon trials ($p=0.006$, $z=2.71$, ranksum=11428) although not compared to Eriksen: $p=0.353$, $z=0.927$, ranksum=11134). (Note that the difference between both and Simon survives Bonferroni correction). Despite the non-significant difference between both conflict trials and Eriksen-only trials, when the effects of either single type of conflict (Eriksen or Simon) are averaged, the effect of both types of conflict occurring together is still larger than the effect of either one ($p=0.012$, $z=2.514$, ranksum=15093).



124
125
126
127
128
129
130
131
132

Figure 1. Multi-source interference task (MSIT) design, recording locations, and behavioral results. (A) Basic task design. Participants fixate on a central cross and then see a visual cue consisting of three numbers and has to identify the unique number with a button push. “correct response” is the left button if the target is 1, middle if 2, right if 3. Four example cues are shown here, and in each case, the target is “2” and the middle button is the correct response. This is most obvious for the first cue (“none”), where there is no conflicting information. In the other three examples, conflicting information makes the task more difficult. First, incongruence between the location of the target number in the 3-digit sequence and

133 location of the correct button in the 3-button pad produces spatial (Simon) conflict (orange).
134 Second, the distracting presence of numbers that are valid button choices (“1”, “2”, “3”)
135 produces flanker (Eriksen) conflict (green). Trials can also simultaneously have both types
136 (blue). B. The visual cues are associated with one or more sensorimotor responses. Every cue
137 has a correct response, meaning the button press that corresponds to the unique target. Cues
138 can also have one or more distractor responses, meaning the button press that corresponds to
139 task-irrelevant spatial information (Simon) or flanking distractors (Eriksen). If and only if the
140 correct response and distractor response do not match, then the cue causes conflict because
141 only one button response can ultimately be chosen. C. Diagram of the intracranial implant
142 showing the UMA and tungsten microelectrode recoding locations schematized as a purple
143 square on the surface of dlPFC. sulcus. D. The average (mean) response times across subjects
144 in each of the four task conditions and (right) the mean response times within each subject.
145 Bars = standard error across subjects.

146

147 **Pre-trial single neuron correlates of conflict**

148 We recorded from 378 neurons from 9 patients in dlPFC. Our goal was to determine
149 whether responses of neurons before the start of the trial predict subsequent reaction time.
150 Consider, first, responses of an example neurons shown in **Figure 2**.

151 In our example neuron (**Figure 2**), taken from dlPFC, both Simon responses and Eriksen
152 responses were significantly greater before the start of faster reaction time trials than before
153 slower reaction time trials (fast Simon RT trials: 3.2 spikes/sec, slow Simon RT trials: 2.5
154 spikes/sec, $p=0.005$, t-test on z-scored data; fast Eriksen RT trials: 3.2 spikes/sec, slow Eriksen
155 RT trials: 2.5 spikes/sec, $p=0.008$, t-test on z-scored data). Specifically, we ran a median split on
156 reaction times post-hoc and separated firing rates on those two categories. As described below,
157 firing rate in this neuron also predicted the reaction time in a continuous model.

158

159 **Pre-trial population correlates of conflict**

160 To explore these effects at the population level, we fit generalized linear models (GLMs)
161 to the pretrial firing rates and reaction times for all trials. Our analyses controlled for prior trial
162 conflict type, because conflict level on the previous trial can modulate preparatory neural
163 responses and lead to trial-to-trial adjustments, such as post-error slowing and conflict-
164 adaptation/trial congruency effects^{19,31,32}. Our analyses also controlled for previous trial reaction
165 time (RT), to remove possible effects of slow drifts in arousal. We analyzed the 500ms epoch
166 between the fixation and cue onset in the current trial.

167 We first asked whether pre-trial activity predicted reaction times on all trials without
168 regard to conflict or history. Pre-trial firing rates in 13.2% of neurons in dlPFC were predictive
169 of the RT on the upcoming trial ($n = 50/378$ neurons). This proportion is greater than that
170 predicted by chance ($p < 0.001$, one-sided binomial test) and remained the same after controlling
171 for prior trial reaction time and conflict type. These results indicate that a small but statistically
172 significant fraction of neurons have firing rates that predict upcoming reaction times.

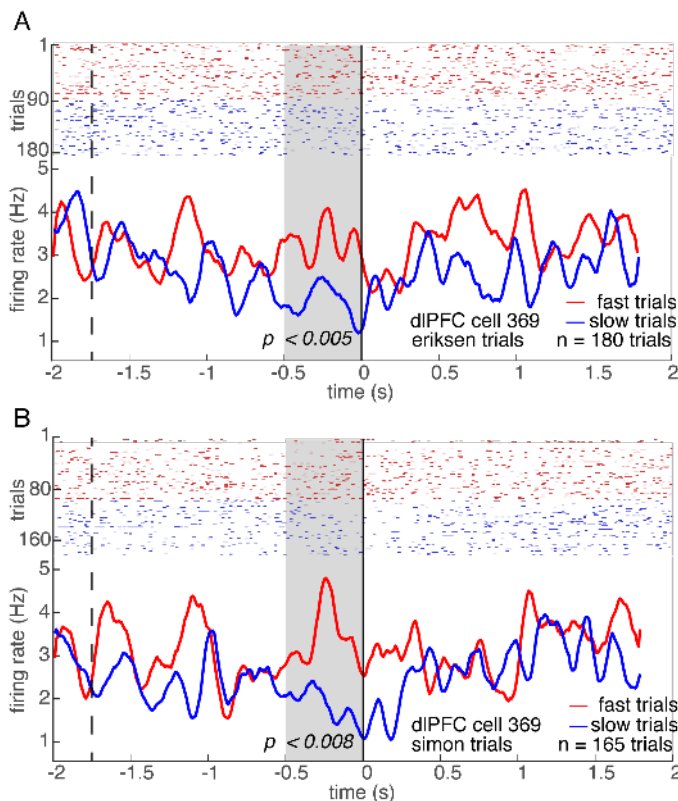
173 After establishing that pretrial activity predicts reaction time overall, we next examined
174 whether it modulated reaction times differently depending on the upcoming conflict condition.
175 We compared a model with a single parameter for any conflict type (“conflict type-amodal”,
176 valued at 1 for any conflict type and 0 for no conflict) to a model with separate parameters for
177 Eriksen and Simon conflict types (“conflict type-specific”), including trials in which the

178 distractor stimuli appeared separately as well as together, and controlling for previous trial
179 conflict and RT. We also compared these models to the “no-conflict” model described above. In
180 both areas, we found significant proportions of cells with a significant main effect of firing rate
181 on response time.

182 At the single cell level, we found evidence for both conflict type-amodal tuning and
183 conflict type-specific tuning. In the conflict type-amodal model, 7.7% of cells exhibited
184 significant single conflict coefficients, a proportion that was significantly greater than chance (n
185 = 29/378, $p = 0.009$, binomial test with chance rate of 5%) and 11.1% of cells showed a main
186 effect (Wald test) of firing rate ($p < 0.001$, one sided binomial test with chance rate of 5%). With
187 the conflict type-specific model, 14.6 % of all cells ($n=55/378$) exhibited significant coefficients
188 (Wald tests) for predicting RT on either Eriksen trials or on Simon Trials ($p < 0.001$, binomial
189 test with chance rate of 9.75%). Examining the main effect of overall firing rate in this model,
190 13.2% of cells showed a significant effect ($n = 50/378$, $p < 0.001$, binomial test).

191 When we examined the evidence for conflict tuning in dlPFC with model comparison, we
192 found that 73% of cells preferred the conflict-specific model ($n = 277/378$, median model 3:1
193 BIC weight ratio = 23, median model 3:2 BIC weight ratio = 40), 22% preferred the no-conflict
194 model ($n = 83/378$, median model 1:3 BIC weight ratio = 2.9, median model 1:2 BIC weight
195 ratio = 44) and only 3% preferred the conflict type-amodal model ($n = 10/378$, median model 2:3
196 BIC weight ratio = 2.8, median model 2:1 BIC weight ratio = 2.4×10^6). Of the 29 cells with
197 significant conflict type-amodal coefficients, 93% ($n = 27/29$) preferred the conflict type-specific
198 model. These BIC results indicate that cells tuned for conflict type-specific responding dominate
199 in dlPFC.

200
201
202



203

204 **Figure 2.** Individual dlPFC neurons signal the speed of upcoming responses in a conflict-specific
205 manner. (A-B) PSTHs of example neuron 369 showing significantly higher pre-trial activity
206 before fast (red) responses than slow (blue) responses in both (A) Eriksen and (B) Simon conflict
207 trials. Gray shading indicates the 500ms analysis window. The dotted line indicates the response
208 on the last trial and the solid vertical line indicates the stimulus onset.

210 **Semi-orthogonal coding for two forms of conflict preparation in dlPFC**

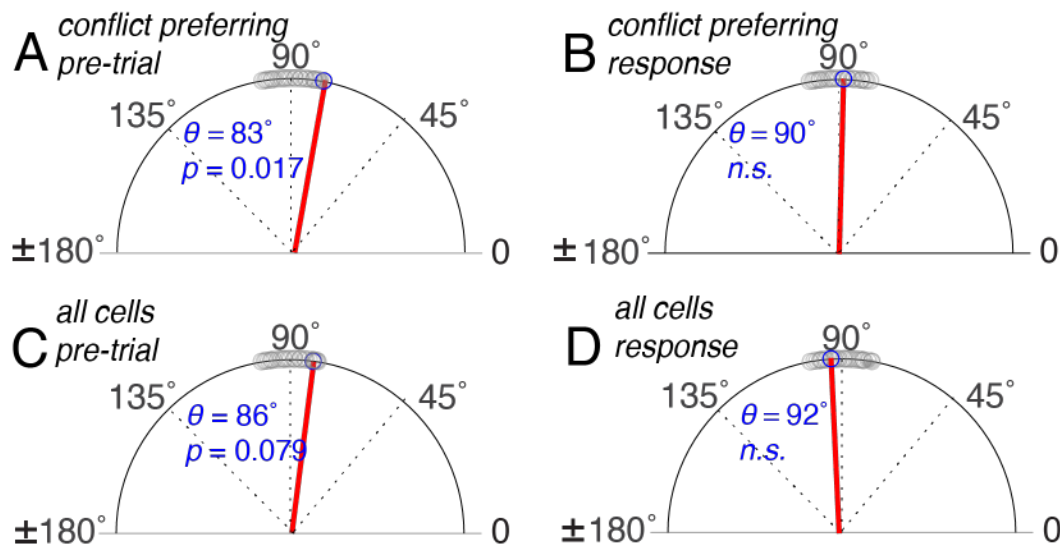
211 Our observation that a significant portion of individual cells code for conflict type-
212 amodal reaction times but yet were mostly better described with the conflict type-specific model
213 led us to wonder if *population-level* activity might contain a conflict type-amodal signal. To test
214 this possibility, we asked how ensemble codes for predicting resolution of Simon and Eriksen
215 conflict, derived from the conflict type-specific model, were related to each other. To do this, we
216 calculated a vector of GLM regression weights for each distractor type across neurons. We call
217 these vectors the *pre-trial tuning weight vectors*. We then compared these vectors by computing
218 the Spearman correlation of the vectors corresponding to Eriksen and Simon coefficients (cf. ³³).
219 (Note that the Spearman test does not assume linearity and is thus more general than the more
220 common Pearson and is also less sensitive to potential outliers). We tested these analyses on all
221 cells that preferred either conflict type-amodal or conflict type-specific models by BIC ($n =$
222 $287/738$) as well as on all cells; doing so allows us to include contributions from all relevant
223 neurons, even those with real effects that do not pass the strict significance threshold; this
224 approach thus has better signal-to-noise (and moderately less susceptible to Type II errors) than
225 analysis approaches that focus on cells that cross a significance threshold (Blanchard et al.,
226 2018).

227 We found that in the conflict-preferring population, the codes for Simon and Eriksen
228 were weakly positively correlated ($\rho = 0.12$, $p = 0.048$; permutation test). Relatedly, we found
229 the angle θ between these vectors to be 83° and significantly less than 90° ($p = 0.017$,
230 permutation test). This result is consistent with the population-level superposition of collinear
231 and orthogonal coding for optimal initial conditions for conflict responding. In the entire
232 population, the angle θ between these vectors was 86° and less than 90° at a trend level ($p =$
233 0.079 , permutation test), and the Spearman's ρ was 0.093 ($p = 0.038$, permutation test). In other
234 words, this result indicates that there is a conflict type-amodal code recoverable from dlPFC
235 ensemble activity.

237 **Firing rates in the response period explain response time variability**

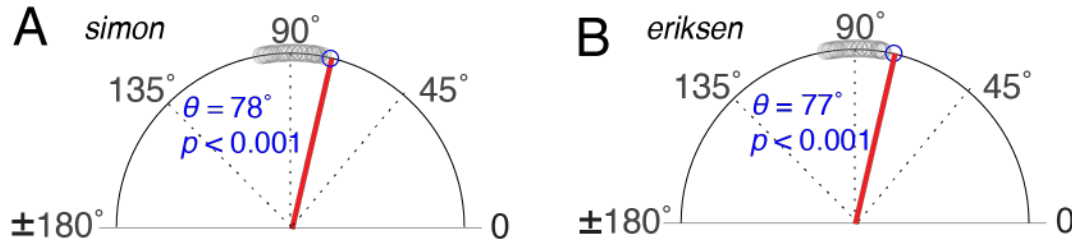
238 If neural firing patterns in the preparatory period bias response speed in a conflict type-
239 specific manner, we would expect the neural state in the response period to reflect this. To test
240 this hypothesis, we ran the conflict type-specific model described above on the 500ms period
241 after stimulus onset. We found that 16.9 % of all cells ($n = 64/378$) exhibited significant
242 coefficients (Wald Test) for predicting RT on either Eriksen trials or Simon Trials ($p < 0.001$,
243 binomial test with chance rate of 9.75%). To examine the degree to which the preparatory state
244 resembled the response state, we computed similarity measures for their respective coding
245 vectors, which we call the *response tuning weight vectors*. For both areas, we found that the pre-
246 trial and response tuning weight vectors were partially co-linear. The Spearman correlation
247 between Eriksen codes for conflict-preferring cells was $r = 0.22$ ($p < 0.001$, permutation test)
248 and between Simon codes was $\rho = 0.23$ ($p < 0.001$, permutation test); the angles were 77° for the
249 Eriksen ($p < 0.001$, permutation test) and 78° for the Simon condition ($p < 0.001$, permutation

250 test). The results for all cells were similar (Eriksen $\rho = 0.22$, $p < 0.001$ and $\theta = 78^\circ$, $p < 0.001$;
 251 Simon $\rho = 0.23$, $p < 0.001$ and $\theta = 75^\circ$, $p < 0.001$). These results support the notion that the
 252 neural states in dlPFC that predispose for more efficient conflict resolution overlap with the
 253 states of efficient responding themselves. Next, we queried the association between the Eriksen
 254 and Simon response tuning weight vectors. We found that the codes for both the conflict-
 255 preferring and all-cell populations were fully orthogonalized in the response period, in contrast to
 256 the pre-trial period (conflict-preferring cells $\rho = -0.01$, $p = 0.882$ and $\theta = 90^\circ$, $p > 0.05$; all
 257 cells $\rho = -0.04$, $p > 0.05$ and $\theta = 92^\circ$, $p > 0.05$, permutation tests). To determine whether the
 258 pre-trial and response correlation coefficients and angles differed, we computed bootstrap
 259 distributions for each and compared the medians. The correlation coefficient for Eriksen versus
 260 Simon pre-trial tuning weight vectors differed significantly from those for the response tuning
 261 weight vectors for both the conflict-preferring population and all cells (Wilcoxon rank sums, all
 262 $p < 0.001$). This is important to confirm because the difference between a significant and non-
 263 significant effect is not necessarily itself significant³⁴.
 264



265
 266

267 **Figure 3.** The angle between conflict-response tuning weight vectors in dlPFC orthogonalizes
 268 between the pre-trial and response period. A zero-degree angle represents complete collinearity.
 269 (A-D) the angle between Eriksen and Simon coding vectors (blue circle, blue numbering and red
 270 line). The significance of the difference from a 90° (blue italics) was computed from permutation
 271 testing. The null distribution is shown with grey circles. (A) Vector angle between conflict
 272 preferring cells (amodal or conflict-type specific) showing superimposed collinear and
 273 orthogonal coding. (B) The angle between all cells shows a similar trend. (C) Same as (A) for
 274 response codes, showing purely orthogonal coding. (D) Same as for (B) for response codes,
 275 showing orthogonal coding.



276
277 **Figure 4.** The angle between pre-trial and response conflict-response tuning weight vectors in
278 dIPFC shows partially co-linear coding in dIPFC. A zero-degree angle represents complete
279 collinearity. (A-B) Conflict-preferring coding vector angles (blue circle, blue numbering and red
280 line); the significance of the difference from a 90° (blue italics) was computed from permutation
281 testing (the null distribution is shown with grey circles). (A) the angle between pre-trial and
282 response Eriksen coding vectors shows significant collinearity as does (B) the angle between
283 pre-trial and response Simon coding vectors.

284

285

DISCUSSION

286

287

288

289

290

291

292

293

294

295

296

297

298

299

300

301

302

303

304

305

306

307

We examined the responses of single neurons in human dIPFC during a task that interleaved two kinds of conflict, Simon and Eriksen. We found that firing rates of a modest but significant proportion of neurons in both areas before the trial predicts the efficiency of cognitive control, as inferred from reaction times. The fact that ensemble responses predict reaction time before the trial, and presumably task-driven cognition, supports the hypothesis that successful cognitive control reflects, in part, the ability to transition through specific brain states. By controlling for prior trial condition and reaction time, we showed that these brain states do not simply reflect adaptation or drifts in arousal, but rather history-independent patterns that predispose to efficient responding.

We also compared the patterns that predicted the efficiency of upcoming responses on trials with either Simon, Eriksen or both types of conflict. At the individual cell level, we found that these responses were consistent with three types of codes: a conflict-independent (no-conflict), a conflict type-amodal and conflict type-specific code. At the population level, we found a weak general conflict type-amodal code. These results demonstrate, first, that neurons in dIPFC process both type-specific and domain-general neural computations. While the domain-general element was observed both at the individual cell level and the population level, model comparison suggests it is more likely a population level phenomenon: in most cells the full model with separate conflict terms significantly outperformed a model with one single term for any type of conflict. A sizable proportion of individual cells (22%) did prefer a model with no conflict term, predicting response speed across all conditions. However, the domain-general/conflict type-amodal element emerged at the population level from the correlation between the conflict-specific regression coefficients across neurons.

308 Studies of motor control in rodents and non-human primates have shown that variability
309 in the firing rates of neurons in motor cortex during movement preparation predicts variability in
310 subsequent movements^{6,9,10}. This body of work has given rise to the “initial condition
311 hypothesis”, which posits that neural firing patterns behave like dynamical systems, and the
312 trajectory of neural dynamics therefore depends on the initial state of the system^{3,8,35}. One
313 implication of this theory is that preparatory neural states can therefore be optimized to
314 efficiently produce a desired behavioral outcome³⁶. If similar principles apply to neural
315 dynamics during cognitive tasks, this suggests that preparatory activity may also be optimized to
316 support the efficient application of cognitive control, consistent with the notion of pro-active
317 control³⁷.

318 Indeed, a growing literature suggests neural patterns subserving cognition are also
319 consistent with dynamical systems models³⁸. Using the same task studied, here, we recently
320 showed that neural population activity in prefrontal regions during conflict resolution follows
321 low-dimensional trajectories that differ depending on the type of conflict²⁸. The divergence of
322 these trajectories raises the question of whether they have different optimal initial states, or if
323 similar neural starting conditions give rise to similar task performance. The results we present
324 provide a somewhat nuanced answer: the optimal initial states overlap slightly, suggesting a
325 weak mechanism for shared conflict-responding, but orthogonalize over the course of response,
326 supporting the notion of trajectory divergence.

327 What are the implications of preparatory brain states for conflict resolution? One
328 possibility is that initial states that predict response times reflect changes in arousal or attention
329 that are either spontaneous or the result of adaptations to the previous trial. While attractive for
330 its simplicity, this explanation would not explain the persistence of the effect after controlling for
331 trial history nor would it explain the conflict type-specific nature of the initial states. Rather, our
332 results suggest that the computations that perform conflict resolution are not only distinct, as
333 implied by the divergent neural state space trajectories, but are facilitated with both shared and
334 independent factors. In this task, participants do not have knowledge of whether the upcoming
335 trial will have one form of conflict or the other or both. Maintaining both shared and independent
336 preparatory factors for conflict types, independent of the past, may allow the brain to respond
337 flexibly to unpredictable challenges while minimizing interference between the processes needed
338 to respond to those challenges. Such a factorized model of representation has been proposed as a
339 mechanism to minimize interference and facilitate generalization in learning³⁹. Why would
340 preparatory states vary from trial to trial? The simplest explanation is spontaneous fluctuations
341 due to noise. Another possibility is that participants are subtly making predictions about the
342 condition of the upcoming trial, perhaps based on longer trial history than the recent past
343 controlled for here.

344 Recent years have seen the emergence of the dynamical systems perspective in motor
345 neurophysiology. This view sees the aggregate activity of neurons in a region as constituting a
346 state and that the execution of motor actions is driven by the lawful progression across states in
347 motor regions. It has been further proposed that cognitive performance may reflect a similar
348 dynamical system view, however, this view has been difficult to test. We recently demonstrated
349 that, in asynchronous choice, neurons in two core reward areas show subspace orthogonalization,
350 a neural process previously associated only with motor cortex⁴⁰. Here we sought to test a critical
351 prediction of the initial state hypothesis. In the motor cortex, the *initial state hypothesis* holds
352 that successful implementation of a motor actions cannot begin until motor cortex enters into a
353 specific ensemble state, defined in practice as an ensemble firing rate pattern. We hypothesized

354 that an analogous idea in cognition would be that implementation of a cognitive act would
355 require implementation of an initial state. Our results suggest that not only does the initial state
356 of neural activity prior to the cognitive act of conflict resolution support efficient responding in a
357 pro-active manner ³⁷, it does so in a largely conflict type-specific manner. The small degree of
358 collinearity we observe in dlPFC may contribute to untangling of stimulus-action processes
359 before full orthogonalization during implementation. Previous work in premotor cortex has
360 shown that the neural state space during responding predicts reaction times in motor tasks ⁴¹. We
361 found that these optimal initial states share structure with the optimal responding states,
362 suggesting they support optimal response trajectories. Future studies may examine whether
363 neural state-space trajectories separate by response time differently depending on both the initial
364 states and the specific cognitive computations the brain performs.

365
366
367
368
369

METHODS

370

371

372 Subjects and ethics statement

373

374 We studied one cohort of 9 patients: 8 (2 female) with movement disorders (Parkinson's disease
375 or essential tremor) who were undergoing deep brain stimulation (DBS) surgery, and one male
376 patient with epilepsy undergoing intracranial seizure monitoring. The entry point for the
377 trajectory of the DBS electrode is typically in the inferior portion of the superior frontal gyrus or
378 superior portion of the middle frontal gyrus, within 2 cm of the coronal suture. This area
379 corresponds to dlPFC (Brodmann's areas 9 and 46). The single epilepsy patient in this cohort
380 underwent a craniotomy for placement of subdural grid/strip electrodes in a prefrontal area
381 including dlPFC.

382 All decisions regarding sEEG and DBS trajectories and craniotomy location were made solely
383 based on clinical criteria. The Columbia University Medical Center Institutional Review Board
384 approved these experiments, and all subjects provided informed consent prior to participating in
385 the study.

386 Behavioral Task

387 All subjects performed the multi-source interference task (MSIT; [Figure 1A](#)). In this task, each
388 trial began with a 500-millisecond fixation period. This was followed by a cue indicating
389 the *correct response* as well as the *distractor response*. The cue consisted of three integers
390 drawn from {0, 1, 2, 3}. One of these three numbers (the "*correct response cue*") was different
391 from the other two numbers (the "*distractor response cues*"). Subjects were instructed to
392 indicate the identity of the correct response number on a 3-button pad. The three buttons on this
393 pad corresponded to the numbers 1 (left button), 2 (middle) and 3 (right), respectively.
394 The MSIT task therefore presented two types of conflict. Simon (motor spatial) conflict occurred
395 if the correct response cue was located in a different position in the cue than the corresponding
396 position on the 3-button pad (e.g. '0 0 1'; target in right position, but left button is correct
397 choice). Eriksen (flanker) conflict occurred if the distractor numbers were possible button
398 choices (e.g. '3 2 3', in which "3" corresponds to a possible button choice; vs. '0 2 0', in which
399 "0" does not correspond to a possible button choice).

400 After each subject registered his or her response, the cue disappeared, and feedback appeared.
401 The feedback consisted of the target number, but it appeared in a different color. The duration of
402 the feedback was variable (300 to 800 milliseconds, drawn from a uniform distribution therein).
403 The inter-trial interval varied uniformly randomly between 1 and 1.5 seconds.

404 The task was presented on a computer monitor controlled by the Psychophysics Matlab Toolbox
405 (www.psychtoolbox.org; The MathWorks, Inc). This software interfaced with data acquisition
406 cards (National Instruments,) that allowed for synchronization of behavioral events and neural
407 data with sub-millisecond precision.

408 Data Acquisition and preprocessing

409 Single unit activity (SUA) was recorded from a combination of two techniques. The DBS
410 surgeries were performed according to standard clinical procedure, using clinical microelectrode
411 recording (Frederick Haer Corp.). Prior to inserting the guide tubes for the clinical recordings,
412 we placed the microelectrodes in the cortex under direct vision to record from dlPFC, (IRB-
413 AAAK2104). The epilepsy implant in Cohort 2 included a Utah-style microelectrode array
414 (UMA) implanted in dlPFC (IRB-AAAB6324). In all cases, data were amplified, high-pass
415 filtered, and digitized at 30 kilosamples per second on a neural signal processor (Blackrock
416 Microsystems, LLC).

417 SUA data were re-thresholded offline at negative four times the root mean square of the 250 Hz
418 high-pass filtered signal. Well-isolated action potential waveforms were then segregated in a
419 semi-supervised manner using the T-distribution expectation-maximization method on a feature
420 space comprised of the first three principal components using Offline Sorter (OLS) software
421 (Plexon Inc, Dallas, TX; USA). The times of threshold crossing for identified single units were
422 retained for further analysis.

423 Data Analysis

424
425 We determined the effect variations in pre-stimulus firing rates had on reaction times by
426 comparing four generalized linear models. We first fit gamma distributions to the reaction times
427 and excluded reaction times with a less than 0.005 probability following ⁴². For each model, we
428 centered and scaled the continuous predictor variables (firing rate and reaction time) by z-
429 scoring. We analyzed correct and incorrect trials to prevent false-positives from data-censoring
430 effects. We pre-selected the pre-trial analysis interval as the 500ms period between fixation and
431 stimulus onset and the response analysis interval as the 500ms following stimulus onset. To
432 determine the overall effect of firing rate marginalized over condition, we first fit the following
433 generalized linear model:

$$434 \quad RT \sim \beta_0 + \beta_1 \overline{FR}$$

437 We then compared several alternative models, while controlling for reaction time and prior
438 conflict: a single firing rate coefficient for all trials model,

$$RT \sim \beta_0 + \beta_1 FR + pC + pRT$$

439 a model with an additional term for the firing rate on trials with any conflict (Simon, Eriksen or
440 both),

$$441 \quad RT \sim \beta_0 + \beta_1 FR + \beta_2 FR * C + C + pC + \overset{441}{\underset{443}{pRT}}$$

445 and a model with separate, additive conflict terms for Simon and Eriksen conditions,

$$446 \quad RT \sim \beta_0 + \beta_1 FR + \beta_2 FR * C_E + \beta_3 FR * C_S + C_E + C_S + pC + pRT$$

448
449 where FR is firing rate on all trials, C is an indicator variable for trials with any conflict, CE and
450 CS are indicator variables for Eriksen and Simon trials, respectively, pC is a categorical variable
451 for prior conflict type and pRT is the previous trial reaction time. We used a normal distribution
452 with a log link function because the reaction time data was well described by a log-normal
453 distribution.

454
455 We compared these models by their BIC weight ratios⁴³. We identified the best fitting model
456 for each cell as the model with a greater than one BIC weight ratio for all pairwise comparisons.
457 The BIC penalty for model complexity is greater than that for Akaike Information Criteria (AIC)
458 as the number of model parameters exceeds $e^2 \sim 7$ and thus more appropriate here (and more
459 conservative)^{43,44}. To assess the significance of overall model fits we performed deviance tests
460 relative to a constant model. To assess the significance of coefficients we performed Wald tests
461 (REF).

462
463 To compare the neural codes for conflict, we entered the regression coefficients into individual
464 vectors for each conflict condition. We then computed the Spearman correlation between those
465 vectors as well as the angle between the vectors. We excluded points more than 3 median
466 absolute deviations from the median because angle measurements; this approach excluded 6
467 cells. We then randomized the vector entries and computed correlations between the randomized
468 vectors to form null distributions (2000 permutations). We computed p-values for the real
469 measurement relative to the corresponding null distribution (permutation test). To compare
470 angles and correlations, we constructed bootstrap distributions with resampling (5000 samples)
471 and compared the medians of the resultant distributions with the non-parametric Wilcoxon rank
472 sum test.

- 473
474
475
476 1. Weissman, D. H., Roberts, K. C., Visscher, K. M. & Woldorff, M. G. The neural bases of
477 momentary lapses in attention. *Nat. Neurosci.* **9**, 971–978 (2006).
- 478 2. Boly, M. *et al.* Baseline brain activity fluctuations predict somatosensory perception in
479 humans. *Proc. Natl. Acad. Sci. U. S. A.* **104**, 12187–12192 (2007).
- 480 3. Churchland, M. M. *et al.* Stimulus onset quenches neural variability: a widespread cortical
481 phenomenon. *Nat. Neurosci.* **13**, 369–378 (2010).
- 482 4. Pezzulo, G. & Cisek, P. Navigating the Affordance Landscape: Feedback Control as a
483 Process Model of Behavior and Cognition. *Trends Cogn. Sci.* **20**, 414–424 (2016).

- 484 5. Riehle, A. & Requin, J. Monkey primary motor and premotor cortex: single-cell activity
485 related to prior information about direction and extent of an intended movement. *J.*
486 *Neurophysiol.* **61**, 534–549 (1989).
- 487 6. Churchland, M. M., Yu, B. M., Ryu, S. I., Santhanam, G. & Shenoy, K. V. Neural
488 variability in premotor cortex provides a signature of motor preparation. *J. Neurosci.* **26**,
489 3697–3712 (2006).
- 490 7. Churchland, M. M., Cunningham, J. P., Kaufman, M. T., Ryu, S. I. & Shenoy, K. V.
491 Cortical preparatory activity: representation of movement or first cog in a dynamical
492 machine? *Neuron* **68**, 387–400 (2010).
- 493 8. Shenoy, K. V., Sahani, M. & Churchland, M. M. Cortical control of arm movements: a
494 dynamical systems perspective. *Annu. Rev. Neurosci.* **36**, 337–359 (2013).
- 495 9. Afshar, A. *et al.* Single-trial neural correlates of arm movement preparation. *Neuron* **71**,
496 555–564 (2011).
- 497 10. Pandarinath, C. *et al.* Inferring single-trial neural population dynamics using sequential
498 auto-encoders. *Nat. Methods* **15**, 805–815 (2018).
- 499 11. Becket Ebitz, R. & Hayden, B. Y. The population doctrine revolution in cognitive
500 neurophysiology. *arXiv [q-bio.NC]* (2021).
- 501 12. Churchland, A. K., Kiani, R. & Shadlen, M. N. Decision-making with multiple alternatives.
502 *Nat. Neurosci.* **11**, 693–702 (2008).
- 503 13. Pastor-Bernier, A. & Cisek, P. Neural Correlates of Biased Competition in Premotor
504 Cortex. *Journal of Neuroscience* vol. 31 7083–7088 (2011).
- 505 14. Yoo, S. B. M. & Hayden, B. Y. Economic Choice as an Untangling of Options into Actions.
506 *Neuron* **99**, 434–447 (2018).

- 507 15. Hunt, L. T. & Hayden, B. Y. A distributed, hierarchical and recurrent framework for
508 reward-based choice. *Nat. Rev. Neurosci.* **18**, 172–182 (2017).
- 509 16. Smith, E. H. *et al.* Widespread temporal coding of cognitive control in the human prefrontal
510 cortex. *Nat. Neurosci.* **22**, 1883–1891 (2019).
- 511 17. Ebitz, R. B. & Platt, M. L. Neuronal activity in primate dorsal anterior cingulate cortex
512 signals task conflict and predicts adjustments in pupil-linked arousal. *Neuron* **85**, 628–640
513 (2015).
- 514 18. Bryden, D. W. *et al.* Single Neurons in Anterior Cingulate Cortex Signal the Need to
515 Change Action During Performance of a Stop-change Task that Induces Response
516 Competition. *Cereb. Cortex* **29**, 1020–1031 (2019).
- 517 19. Sheth, S. A. *et al.* Human dorsal anterior cingulate cortex neurons mediate ongoing
518 behavioural adaptation. *Nature* **488**, 218–221 (2012).
- 519 20. Shenhav, A. *et al.* Toward a Rational and Mechanistic Account of Mental Effort. *Annu. Rev.*
520 *Neurosci.* **40**, 99–124 (2017).
- 521 21. Yeung, N., Holroyd, C. B. & Cohen, J. D. ERP correlates of feedback and reward
522 processing in the presence and absence of response choice. *Cereb. Cortex* **15**, 535–544
523 (2005).
- 524 22. Botvinick, M. M., Braver, T. S., Barch, D. M., Carter, C. S. & Cohen, J. D. Conflict
525 monitoring and cognitive control. *Psychol. Rev.* **108**, 624–652 (2001).
- 526 23. Botvinick, M. M. & Cohen, J. D. The Computational and Neural Basis of Cognitive
527 Control: Charted Territory and New Frontiers. *Cognitive Science* vol. 38 1249–1285 (2014).
- 528 24. Miller, E. K. & Cohen, J. D. An integrative theory of prefrontal cortex function. *Annu. Rev.*
529 *Neurosci.* **24**, 167–202 (2001).

- 530 25. MacDonald, A. W., 3rd, Cohen, J. D., Stenger, V. A. & Carter, C. S. Dissociating the role
531 of the dorsolateral prefrontal and anterior cingulate cortex in cognitive control. *Science* **288**,
532 1835–1838 (2000).
- 533 26. Shenhav, A., Botvinick, M. M. & Cohen, J. D. The expected value of control: an integrative
534 theory of anterior cingulate cortex function. *Neuron* **79**, 217–240 (2013).
- 535 27. Johnston, K., Levin, H. M., Koval, M. J. & Everling, S. Top-down control-signal dynamics
536 in anterior cingulate and prefrontal cortex neurons following task switching. *Neuron* **53**,
537 453–462 (2007).
- 538 28. Becket Ebitz, R. *et al.* Human dorsal anterior cingulate neurons signal conflict by
539 amplifying task-relevant information. *Cold Spring Harbor Laboratory* 2020.03.14.991745
540 (2020) doi:10.1101/2020.03.14.991745.
- 541 29. Bush, G., Shin, L. M., Holmes, J., Rosen, B. R. & Vogt, B. A. The Multi-Source
542 Interference Task: validation study with fMRI in individual subjects. *Mol. Psychiatry* **8**, 60–
543 70 (2003).
- 544 30. Deng, Y., Wang, X., Wang, Y. & Zhou, C. Neural correlates of interference resolution in
545 the multi-source interference task: a meta-analysis of functional neuroimaging studies.
546 *Behav. Brain Funct.* **14**, 8 (2018).
- 547 31. Horga, G. *et al.* Adaptation to conflict via context-driven anticipatory signals in the
548 dorsomedial prefrontal cortex. *J. Neurosci.* **31**, 16208–16216 (2011).
- 549 32. Oehr, C. R. *et al.* Neural communication patterns underlying conflict detection, resolution,
550 and adaptation. *J. Neurosci.* **34**, 10438–10452 (2014).

- 551 33. Blanchard, T. C., Hayden, B. Y. & Bromberg-Martin, E. S. Orbitofrontal cortex uses
552 distinct codes for different choice attributes in decisions motivated by curiosity. *Neuron* **85**,
553 602–614 (2015).
- 554 34. Nieuwenhuis, S., Forstmann, B. U. & Wagenmakers, E.-J. Erroneous analyses of
555 interactions in neuroscience: a problem of significance. *Nat. Neurosci.* **14**, 1105–1107
556 (2011).
- 557 35. Ames, K. C. & Churchland, M. M. Motor cortex signals for each arm are mixed across
558 hemispheres and neurons yet partitioned within the population response. *Elife* **8**, (2019).
- 559 36. Kao, C.-H., Lee, S., Gold, J. I. & Kable, J. W. Neural encoding of task-dependent errors
560 during adaptive learning. *Elife* **9**, (2020).
- 561 37. Braver, T. S. The variable nature of cognitive control: a dual mechanisms framework.
562 *Trends Cogn. Sci.* **16**, 106–113 (2012).
- 563 38. Taghia, J. *et al.* Uncovering hidden brain state dynamics that regulate performance and
564 decision-making during cognition. *Nature Communications* vol. 9 (2018).
- 565 39. Behrens, T. E. J. *et al.* What Is a Cognitive Map? Organizing Knowledge for Flexible
566 Behavior. *Neuron* **100**, 490–509 (2018).
- 567 40. Yoo, S. B. M. & Hayden, B. Y. The Transition from Evaluation to Selection Involves
568 Neural Subspace Reorganization in Core Reward Regions. *Neuron* **105**, 712-724.e4 (2020).
- 569 41. Michaels, J. A., Dann, B., Intveld, R. W. & Scherberger, H. Predicting Reaction Time from
570 the Neural State Space of the Premotor and Parietal Grasping Network. *J. Neurosci.* **35**,
571 11415–11432 (2015).
- 572 42. Widge, A. S. *et al.* Deep brain stimulation of the internal capsule enhances human cognitive
573 control and prefrontal cortex function. *Nat. Commun.* **10**, 1536 (2019).

- 574 43. Wagenmakers, E.-J. & Farrell, S. AIC model selection using Akaike weights. *Psychon.*
575 *Bull. Rev.* **11**, 192–196 (2004).
- 576 44. *Model Selection and Multimodel Inference: A Practical Information-Theoretic Approach.*
577 (Springer, New York, NY, 2002).